Two-Dimensional ^{13}C Magic Angle Turning NMR Analyses of Dynamics in Poly(2-hydroxypropyl ether of bisphenol A)

Hironori Kaji,* Kazunori Fuke, and Fumitaka Horii

Institute for Chemical Research, Kyoto University, Uji, Kyoto 611-0011, Japan

Received January 16, 2003

ABSTRACT: Two-dimensional solid-state ^{13}C magic angle turning (MAT) NMR spectroscopy, for measuring and separating the line shapes of chemical shift anisotropy (CSA) in respective ^{13}C species, has been applied to the study of dynamics in amorphous poly(2-hydroxypropyl ether of bisphenol A) (PHR). From the temperature dependence of the CSA line shapes, the flip motion of the phenylene ring is quantitatively analyzed; the phenylene ring undergoes a π-flip motion with standard deviations, σ, of 25° and 30−35° at 27 and 90 °C, respectively. Accompanying the flip motion, the main-chain fluctuational motion is revealed from the temperature dependence of the CSA line shapes of the phenylene ring quaternary carbons. The cone angle of the main-chain fluctuation is 10−15° and 12−20° at 27 and 90 °C, respectively. On the basis of the main-chain motion, we propose a model to account for the coincidences of the frequencies and the activation energies of the phenylene ring π-flip motion and γ-relaxation. In the model, the main-chain fluctuation is activated by the phenylene ring π-flip motion in the neighboring chains, which would be the origin of the mechanical γ-relaxation.

Introduction

In our previous paper,[1] the dynamics of an amorphous linear polymer, poly(2-hydroxypropyl ether of bisphenol A), known as phenoxy resin (PHR), was investigated by solid-state one- and two-dimensional cross-polarization/magic angle spinning (CP/MAS) NMR experiments. The frequencies of motion can be determined over a wide temperature range, including α and γ relaxations, observed at 70 to 100 °C and −100 to −40 °C, respectively.[2,3] The α-relaxation corresponds to the glass transition and is found to be related to the main-chain dynamics. In contrast, the molecular origin of mechanically detected γ-relaxation, sometimes called secondary relaxation, is still controversial. This is because mechanical relaxation measurements cannot identify the molecular origin. Other techniques, such as dielectric relaxation and NMR measurements, can characterize the molecular origin. However, the motions characterized by these techniques are not necessarily related to mechanically active relaxations.

The measurements of ^{13}C chemical shift anisotropy (CSA) in solid-state NMR are useful for characterizing the geometry and amplitude of motion in detail for the respective carbon sites which are lost in MAS experiments. The ^{13}C CSA spectra of solid polymers are easily measured by CP/dipolar decoupled experiments without MAS, if the polymer contains only a single ^{13}C site. However, multiple ^{13}C sites exist in most polymers, and the respective CSA spectra should be separated to carry out the detailed analyses; otherwise, the overlap of the respective CSA spectra makes the analysis difficult and unreliable.

Although various techniques[4−18] have been developed for the separation of respective CSA powder patterns, most of the techniques require mechanically demanding special hardware[4,5,7−12] or need special care and sophistication in setting up the radio-frequency pulses because of the sensitivity to pulse-length imperfections and off-resonance effects.[13] Among them, the two-dimensional magic angle turning (2D MAT) technique, originally realized by Gan[6] and further developed mainly by Hu et al.,[15−18] can separate the CSA line shapes by standard NMR hardware without using special probes and isotopic labeling of samples. In the 2D MAT experiments, sample rotation frequencies should be ultraslow (approximately below 100 Hz for 300 MHz NMR spectrometers). The only difficulty in the 2D MAT experiments is maintaining the rotation frequency stable during the experiments, and this has been accomplished within 1 Hz at ambient temperature.[6,15−19] For the study of dynamics, variable temperature experiments are desired, and maintaining the rotation frequency stable over wide temperature ranges, especially at low temperatures, is challenging. Moreover, this 2D MAT technique does not scale the CSA spectra, and a detailed analysis for small-angle fluctuation can be carried out, which is found to be important for the present purpose as shown later.

In this paper, 2D MAT experiments at different temperatures were carried out to measure the CSA line shapes of the respective ^{13}C species. The temperature dependences of the CSA spectra thus obtained were analyzed by two-, four-, and eight-site exchange models to provide the details of the dynamics in PHR. The intermolecular cooperative motion below the glass transition temperature (T_g) is discussed on the basis of the results of main-chain fluctuation in the glassy state, which is unambiguously obtained from the quaternary carbons in bisphenol A residues.

Experimental Section

Sample. Phenoxy resin (PHR) films (Union Carbide, grade PKHJ), used in this work, was prepared by being hot-pressed at 160 °C at 100 kg cm^{-2}, quenched in ice−water, and dried at room temperature under vacuum for 3 days.

NMR Measurements. Solid-state ^{13}C NMR measurements were conducted on a Chemagnetics CMX-400 spectrometer operating under a static magnetic field of 9.4 T (^{13}C frequency of 100.28 MHz). The ^{1}H and ^{13}C field strengths $\gamma B_1/2\pi$ of 62.5 kHz were used for 90° pulses and the cross-polarization (CP).

* To whom correspondence should be addressed: e-mail kaji@scl.kyoto-u.ac.jp.

10.1021/ma0300342 CCC: $25.00
Published on Web 05/20/2003

A CP time of 2 ms, an acquisition time of 5.12 ms, a dwell time of 10 μs, and ^{1}H decoupling fields of 50 kHz were used.

For 2D MAT experiments, a triple-echo sheared MAT pulse sequence[15] was used in this work. The τ delays for the triple Hahn echoes were 20 μs. In the t_1 dimension, 64 slices with increments of 30 μs were acquired. The rotation frequencies of the sample were set to 128 ± 1 and 125 ± 1 Hz at 27 and 90 °C, respectively. The rotation frequency for the experiment at −140 °C was 128 ± 1 Hz except when we replaced a N_2 gas tank with a new one. The rotation frequency and temperature became unstable during the exchange of tanks. Although this was a very short time compared to the total experimental time, it could be one of the origins of the artifacts in the 2D MAT spectrum.

Up to now, 2D MAT techniques are mainly applied to low molecular weight organic samples. For these experiments, slower sample rotation frequencies of less than 100 Hz were used because the line widths in the CP/MAS spectra are narrow for these samples. In our case, the sample is an amorphous polymer whose line widths are much greater. Therefore, the CSA line shapes are quite insensitive to the rotation frequencies. The static magnetic field, B_0, is another factor; the spinning speed of 100 Hz in the 300 MHz spectrometer (^{13}C frequency of 75.46 MHz) originally used by Gan[6] corresponds to 133 Hz in the 400 MHz spectrometer (^{13}C frequency of 100.28 MHz) in our case. Therefore, higher rotation frequencies can be utilized in our case.

We should examine the effect of spin−lattice relaxations because the ^{13}C spin−lattice relaxation times, T_{1C}, for amorphous polymers normally exhibit nonexponential decays, and the initial decays are much shorter than those for the rigid low molecular weight organic samples. After each 1/3-evolution time, the magnetization flips back to the z-direction (along the B_0 direction) and should wait until the sample rotates 120°. During the two waiting times in the MAT pulse sequence,[6,15] spin−lattice relaxation could occur. Now, we compare two different rotation frequencies of 50 and 128 Hz, for example. For these rotation frequencies, the maximum waiting times, during the magnetizations along the z-direction, are 40 and 15.6 ms, respectively. From the T_{1C} measurements for PHR between 20 and 100 °C, the magnetization decays are 0, 4, 5, and 14% of the total magnetizations for the duration of 40 ms for quaternary carbons, phenylene ring C−H carbons, CH_2/CH carbons, and CH_3 carbon, respectively. The corresponding decays are reduced to 0, 1, 2, and 5% at the duration of 15.6 ms. Therefore, the higher sample rotation frequency is better to use for minimizing the ^{13}C spin−lattice relaxation effect; otherwise, artifacts would appear, and some fractions of mobile components would be lost in the resulting spectra. The higher rotation frequency is also suitable for the stable rotation at different temperatures.

We tested the dependence of the sample rotation frequencies directly in the 2D MAT experiments at 27 °C. Despite the above-mentioned differences, no detectable differences were found between the spectra obtained by rotation frequencies at 50 and 128 Hz. The distribution of amplitude and/or frequency of motion in amorphous PHR would be another factor to smear out the difference in the experimental spectra.

The temperatures appearing in this paper are the calibrated temperatures by the ethylene glycol method[20,21] and ^{207}Pb measurements.[22,23] ^{13}C chemical shifts were expressed as values relative to tetramethylsilane (Me_4Si) by using the CH_3 resonance line at 17.36 ppm for hexamethylbenzene crystals as an external reference.

Differential Scanning Calorimetry (DSC). DSC measurements were performed on a TA Instruments DSC 2910 differential scanning calorimeter at a heating rate of 10 °C min^{-1}. Indium was used as a standard for temperature calibration. The T_g determined from the onset and the midpoint of the heat capacity increment were 80 and 87 °C, respectively. No other obvious exothermic and endothermic peaks were observed between −100 and 200 °C.

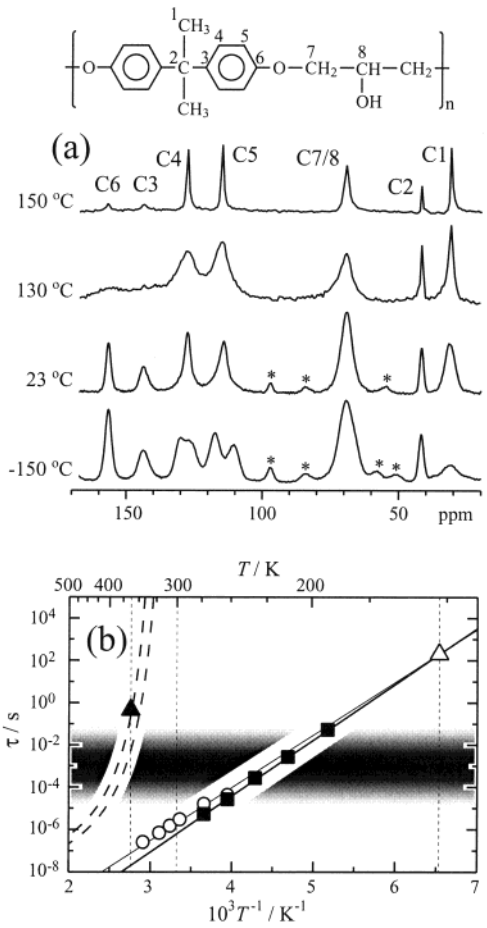

Figure 1. (a) CP/MAS ^{13}C NMR spectra of phenoxy resin (PHR) from −150 to 150 °C. The sign * indicates spinning sidebands. (b) The Arrhenius plot for the correlation time of motion associated with the α and γ relaxations of PHR. Broken lines: motional broadening; ▲, 2D exchange at 90 °C; △, 2D exchange at −120 °C; ■ and thick solid line, two-site exchange with KWW β = 0.2 in which flip angle distributions are considered according to the results of the 2D exchange; ○ and thin solid line, ^{2}H NMR.[24] The frequency region, which can be analyzed by the following ^{13}C CSA spectra, is shown as a shaded region.

Results

Frequency of Motion Analyzed from CP/MAS ^{13}C NMR Spectra. First of all, we summarize our previous results on solid-state one- and two-dimensional CP/MAS NMR experiments.[1] Figure 1a shows the CP/MAS ^{13}C NMR spectra of PHR at different temperatures ranging from −150 to 150 °C. The assignment of each resonance line has been done on the basis of the results of the solution-state ^{13}C NMR spectrum. The splitting of both the resonances of the C−H carbons of the phenylene rings (C4 and C5) into two resonance lines, each at −150 °C, indicates that each of the phenylene C−H carbons exists in a magnetically distinct site at lower temperatures and that the coalescence of the resonance lines at elevated temperatures is caused by the phenylene ring motion. The frequency of this motion, which corresponds to γ-relaxation, is distributed, and the spectra are analyzed on the assumption of KWW function, $\exp(-(t/\tau)^{\beta})$, for the distribution. The average correlation times, τ, thus obtained are shown in Figure 1b as filled squares. The dynamics of γ-relaxation was also investigated by ^{2}H NMR (open circles in Figure 1b).[24] These one-dimensional (1D) ^{13}C and ^{2}H NMR

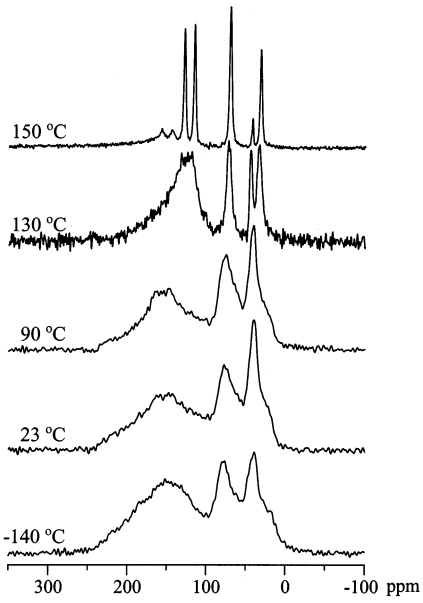

Figure 2. 1D static ^{13}C NMR spectra of PHR from −140 to 150 °C. CSA line shapes are severely overlapped, in particular for the phenylene ring carbons, at low temperatures. 128 scans (from −140 to 90 °C) and 256 scans (for 130 and 150 °C) are acquired.

results are consistent except for the distribution width; the values of KWW-β of 0.2 and 0.6 are assumed in our previous paper[1] and in Shi's paper,[24] respectively. In our case, the value of $\beta = 0.2$ is determined by the mixing time dependence of exchange signal intensities in the 2D CP/MAS ^{13}C NMR experiments.

The broader line width at 130 °C, so-called motional broadening, is caused by main-chain motion, which corresponds to α-relaxation. On the basis of the detailed analyses of the temperature dependence of the resonance lines, the frequencies of motion are quantitatively determined. The results are also shown in the frequency map in Figure 1b as thick broken lines. The results of the 2D CP/MAS ^{13}C NMR experiments, shown by filled and open triangles in Figure 1b, are also consistent with the above-mentioned 1D results. More details are described in our previous paper.[1]

^{13}C CSA Spectra. In Figure 2, the CP/dipolar decoupled spectra of PHR without sample spinning are displayed. Below T_g all the CSA line shapes, in particular, the phenylene ring carbons, are severely overlapped, and the analysis is difficult. At 130 °C, the CSA line shapes are found to be partially averaged. At 150 °C, the respective CSA spectra are well-resolved, and 2D experiments for the separation were unnecessary. The CSA line shapes at 150 °C are Lorentizan and appear at the isotropic chemical shift even without sample spinning. This shows that all the carbons undergo almost isotropic random orientational motion, that is, the isotropic main-chain motion, with a rate above 10^5 Hz at above 150 °C. Note that the CSA line shapes are affected only by local motions. At a longer size range, the motion of polymer chains is found to be anisotropic even in the melt, which originates from chain entanglements in the polymers. See refs 25−29 for the NMR observation of the long-range chain dynamics.

2D MAT Spectra. The CSA line shapes for the respective carbon species, which are overlapped in Figure 2, can be separated using 2D MAT techniques. Figure 3a shows a 2D MAT spectrum of PHR at 90 °C.

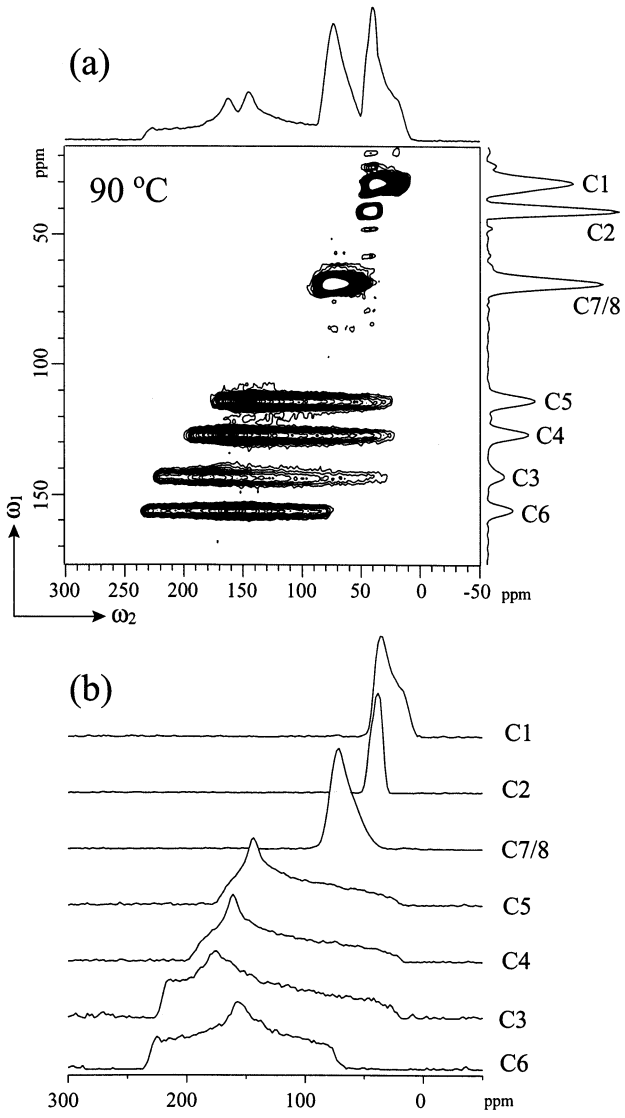

Figure 3. (a) 2D MAT spectral contour plots and the sky projections onto the acquisition and evolution dimensions for PHR at 90 °C. Gaussian line broadenings of 200 Hz were applied along both dimensions. Thirty contour lines are plotted between 2 and 40% of the maximum intensity. (b) CSA spectra thus obtained for the respective carbon species.

The "sky projections", plots of the highest point in each row or column, of the 2D spectrum are also shown for both dimensions. The high-resolution spectra equivalent to the CP/MAS spectra in Figure 1 can be obtained in the projection in the ω_1 dimension. It should be noted that the projection in the ω_1 dimension shows a sideband-free spectrum at such an ultraslow spinning speed. This is an advantage for forthcoming high-field magnets, where high spinning speeds are necessary to obtain sideband-free CP/MAS spectra. Furthermore, the difficulty of maintaining the ultraslow spinning speed stable is relieved under the high-field magnet as described above. The respective CSAs, which are overlapped in the ω_2 dimension and in Figure 2, are found to be well-separated in the 2D spectrum. The CSA line shapes for the respective ^{13}C species thus obtained are shown in Figure 3b.

Figure 4 shows the 2D MAT spectra of PHR at 27 and −140 °C. It is found that the 2D experiments at 27 and −140 °C also separate each CSA spectrum. In particular, the split of the C5 carbon at −140 °C was success-

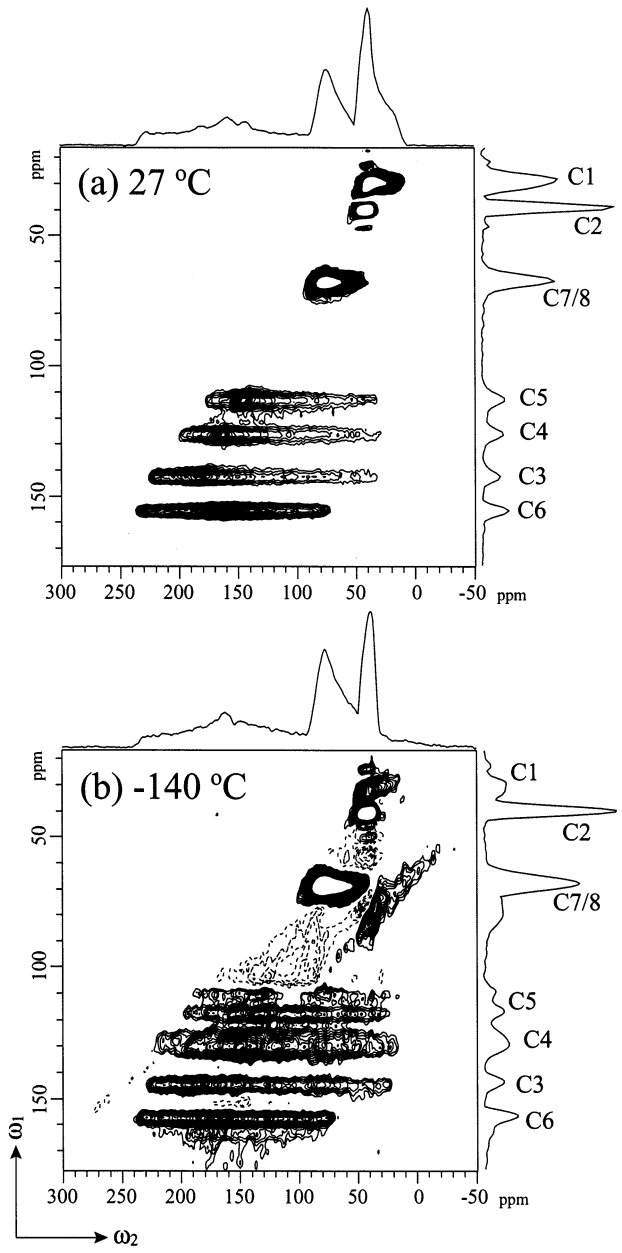

Figure 4. 2D MAT spectral contour plots and the sky projections onto the acquisition and evolution dimensions for PHR at (a) 27 and (b) −140 °C. Gaussian broadenings of 200 Hz were applied along both dimensions. In (a), 30 contour lines are plotted between 3 and 30% of the maximum intensity. In (b), negative artifacts are also shown by dotted lines; of 60 contour lines, 30 are plotted between 3 and 30% of the maximum intensity and 30 between −3 and −30%.

fully obtained. However, positive and negative artifacts appear on the diagonal line in the 2D spectrum in Figure 4b. The artifacts, so-called axial peaks,[30] appear at the center of the ω_1 dimension in the 2D spectrum before shearing and would be caused by instability of the spinning speed and temperature as described in the Experimental Section. The negative artifacts distort the CSA line shapes of the C5 carbons significantly. They are also overlapped on the downfield (σ_{11}) part of the CSA of the C4 carbons. The positive artifacts appear at the C7/8 slice in the ω_1 dimension but are outside the CSA spectrum. The C1, C2, C3, and C6 CSA line shapes are unaffected by the artifacts. In the following quantitative analyses of phenylene ring motion, the C6 and C4 carbons are mainly used.

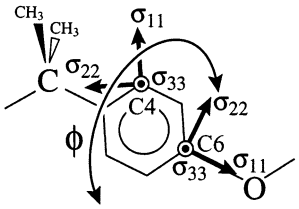

Figure 5. Schematics of the two-site exchange model for phenylene ring flip motion. Principal shielding orientations for the phenylene ring carbons of PHR are also shown.

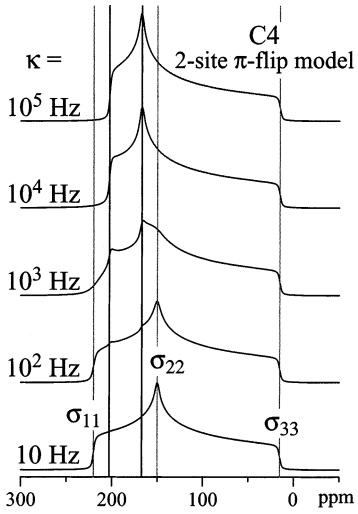

Figure 6. Simulated ^{13}C CSA spectra of C4 carbons under 180°-flip motion. The frequencies of the motion are indicated in the figure. The line shapes below 10 Hz and above 10^5 Hz are insensitive to the frequencies and found to be in the slow and fast limits, respectively.

Analyses of CSA Line Shapes of Phenylene Ring Carbons. Frequency Dependences. In Figure 5, the chemical shift tensor orientations, that is, the orientations of the principal axes,[31] are shown for the phenylene ring carbons of PHR. On the basis of the tensor orientations, the following simulations of CSA line shapes were carried out to obtain quantitative information. The flip frequency dependence of the CSA line shapes under the ideal two-site π-flip motion for the C4 carbon is shown in Figure 6. Below 10^1 Hz and above 10^5 Hz, the changes in the CSA line shapes are indistinguishable, and the flip frequencies are found to be in the slow- and fast-motion limit, respectively.

In general, the CSA line shapes depend on both the frequency and geometry of motion, which sometimes makes the analysis difficult. However, the frequency of motion has already been determined by our previous work[1] and ^2H NMR by Shi et al.[24] (see Figure 1b). Using the previously determined frequency of motion, the quantitative analysis of the geometry of motion can be carried out for CSA spectra obtained by the 2D MAT experiments. The average flip frequency of phenylene ring motion in PHR is extrapolated to be $(1-2) \times 10^{-5}$ Hz at −140 °C (see refs 1 and 24 or Figure 1b). Therefore, the CSA line shapes of phenylene ring carbons are considered to be in the slow limit (in the rigid state) at −140 °C in a good approximation, even though the correlation times are widely distributed.[1,24] All the experimental CSA spectra at −140 °C are reproduced by the static CSA simulation spectra, which will appear later. For the simulation of the C4 carbons at −140 °C, the overlap of artifacts at the σ_{11} part makes

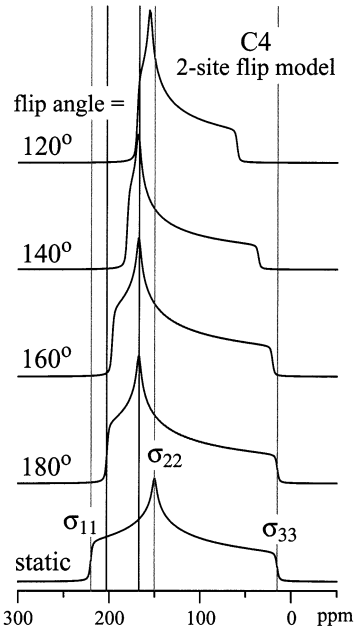

Figure 7. Simulated ^{13}C CSA spectra of C4 carbons under phenylene ring flip motion in the fast limit. The flip angles of the motion are indicated in the figure. The simulated static CSA spectrum is also shown for reference.

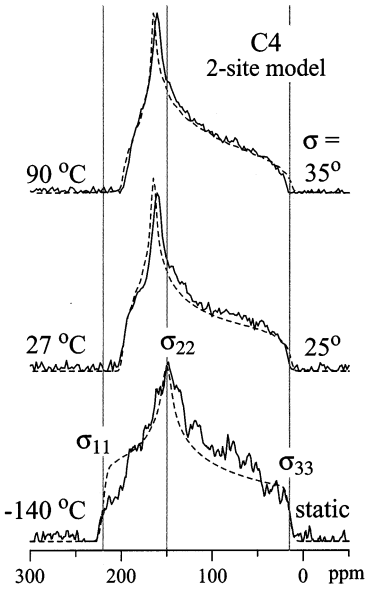

Figure 8. Experimental and simulated ^{13}C CSA spectra of C4 carbons at different temperatures. Here only the Gaussian-distributed phenylene ring flip motion is considered and the simulations with $\sigma = 25$ and 35° give the best-fit simulations for 27 and 90 °C, respectively.

the determination of the value of σ_{11} unreliable (see the bottom of Figure 8). However, the value of σ_{11} is uniquely determined from the isotropic chemical shift, σ_{iso}, and the remaining two principal values, σ_{22} and σ_{33}, according to the relation of $\sigma_{iso} = (\sigma_{11} + \sigma_{22} + \sigma_{33})/3$. The values of ($\sigma_{11}$, σ_{22}, σ_{33}; σ_{iso}) thus obtained for the C4 carbon are (220, 150, 15; 128.3) ppm. The parameter set for the C6 carbon is (235, 162, 68; 155) ppm (see the bottom of Figure 14).

As shown in Figure 1b, the average frequencies of the flip motion at 27 and 90 °C are $(0.5-1) \times 10^6$ and $(1-5) \times 10^7$ Hz, respectively. Therefore, the experimental spectra at these temperatures can be simulated by the spectra in the fast limit in a good approximation.

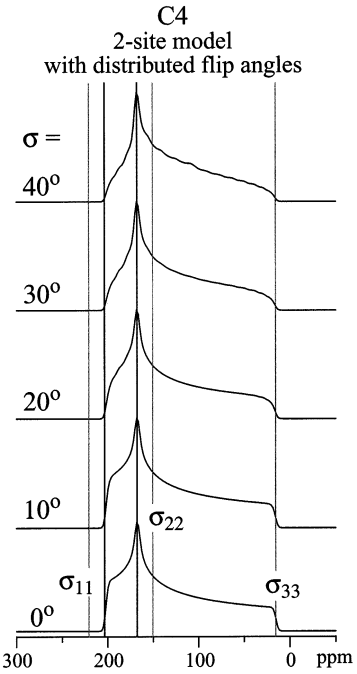

Figure 9. Simulated ^{13}C CSA spectra of C4 carbons under phenylene ring flip motion in the fast limit. For the flip angles, Gaussian distributions with standard deviation, σ, centered at 180° are assumed.

Flip Angle Dependences. Figure 7 shows the simulated spectra under the phenylene ring flip motion for C4 carbons with different flip angles in the fast limit. The ideal 180°-flip motion shows the upfield and downfield shifts of σ_{11} and σ_{22} positions, respectively, whereas σ_{33} is invariant. For the other flip angles, a further upfield shift of σ_{11} and a downfield shift of σ_{33} are observed. The change in the σ_{22} position is negligibly small for the flip angles between 180 and 140°. At 120°, the position of σ_{22} shifts upfield and a significant change in σ_{33} is observed.

Simulations by Flip Angle Distribution. The temperature dependence of the experimental CSA spectra of the C4 carbon is shown in Figure 8 as solid lines. The broken line for the experimental spectrum at −140 °C is the best-fit simulation in the rigid state. The simulation well reproduces the experimental spectrum except for the σ_{11} part, which is due to the overlap of negative artifacts as described above. For the experimental spectra at 27 and 90 °C, the shoulders at σ_{11} and σ_{33} positions are more rounded compared to the simulated spectra in Figure 7. It is therefore found that the experimental spectra could not be accounted for by only a single flip angle. Because PHR is a structurally disordered amorphous polymer, a Gaussian distribution of flip angles centered at 180° is assumed here. The distribution of flip angles with an average angle of 180° was directly proven by 2D ^2H exchange NMR experiments for bisphenol A polycarbonate (BPA-PC)[32] and was assumed for the analyses of motion in PHR in refs 1 and 24. Figure 9 shows the simulated spectra of the C4 carbons by considering the flip angle distribution for phenylene ring flip motion in the fast limit. The widths of the Gaussian distributions are described by the standard deviations, σ. With increasing distribution, the σ_{11} and σ_{33} parts become rounded, and the intensities relative to the intensity at σ_{22} decrease. The chemical shift of σ_{22} is constant irrespective of the distribution up to $\sigma = 40°$. The CSA line shapes in Figure 9 with σ

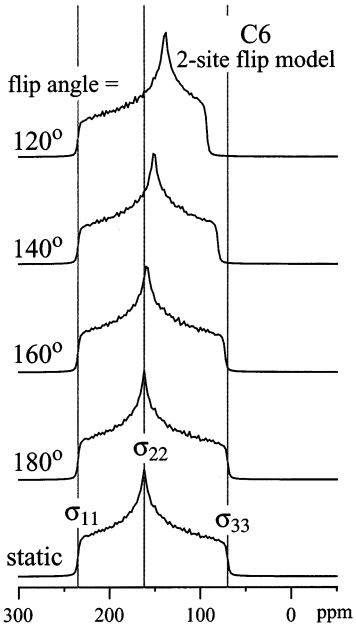

Figure 10. Simulated ^{13}C CSA spectra of C6 carbons under phenylene ring flip motion in the fast limit. The flip angles of the motion are indicated in the figure. The simulated static CSA spectrum is also shown for reference.

= 20−30° appear quite similar to the experimental CSA line shapes at 27 and 90 °C in Figure 8.

The best-fit simulations for the experimental spectra at 27 and 90 °C are shown by the broken lines in Figure 8. The two-site phenylene ring flip motion is considered for the simulations with distributed flip angles centered at 180°. From the best-fit simulations, the distributions of phenylene ring flip angles are determined to be σ = 25 and 35° at 27 and 90 °C, respectively. The coincidences of experimental and simulated spectra appear fine, but a slight inconsistency in the σ_{22} position is observed. As found from Figure 7, the σ_{22} position can be shifted upfield by considering a wider flip angle distribution. However, in this case, a significant downfield shift occurs for σ_{33}, which becomes inconsistent with the σ_{33} position between the experimental and simulated spectra.

Fluctuation of Chain Axis. Figure 10 shows the simulated spectra under the phenylene ring flip motion for the C6 carbons with different flip angles in the fast limit. The line shape under the ideal 180°-flip motion is identical with that of the static CSA. With increasing deviation from 180°, the upfield shift of σ_{22} and downfield shifts of σ_{33} positions are observed. In contrast, σ_{11} is invariant because σ_{11} does not change direction by any flip angles, as shown in Figure 5. Therefore, the motion of the chain axis can be monitored from the change in the σ_{11} positions in the phenylene ring axis carbons exclusively. In Figure 11, the expanded experimental CSA spectra around the σ_{11} regions are shown for the phenylene ring quaternary (C3 and C6) carbons. The slopes of σ_{11} at 90 °C shift upfield by 4−5 ppm compared to those at −140 °C in both spectra. These are definite differences in the NMR experiments in the ^{13}C frequency of 100 MHz, although the shifts are small compared to the CSA widths. These results indicate that the phenylene ring flip axis, that is, the main chain, is fluctuating.

For the simulation of the fluctuational motion of the chain axis, the four-site exchange model is assumed as

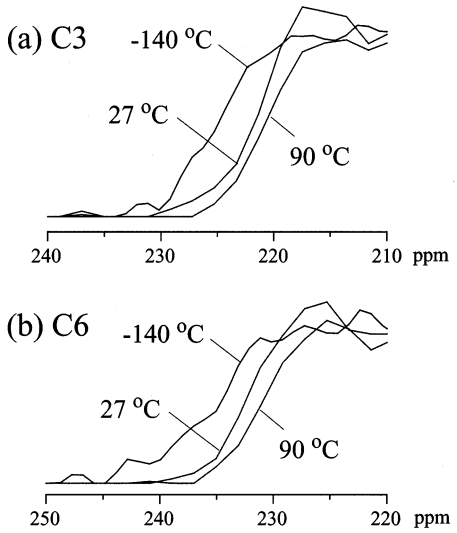

Figure 11. Expansion of σ_{11} shoulders in the experimental CSA spectra of (a) C3 and (b) C6 carbons.

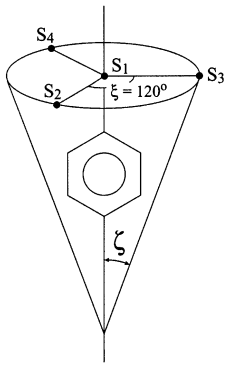

Figure 12. Schematics of four-site exchange model for the fluctuational motion of phenylene ring axes.

shown in Figure 12. Figure 13 shows the change in the C6 CSA line shapes by cone angle, ζ, in the fast limit. The σ_{11} upfield shift is observed in the simulations. Different from the simulations in Figure 10, the chemical shift of σ_{22} is shifted downfield with increasing ζ. In comparison with the expanded CSA spectra in Figure 11, the fluctuating angle, ζ, is found to be around 10°. The chemical shift of σ_{22} for ζ = 10° is almost the same as that of the static spectrum. Therefore, the chemical shifts of σ_{22} in the experimental CSA spectra become good indicators of the phenylene ring flip angle distribution.

Finally, the experimental C6 CSA line shapes at 27 and 90 °C are simulated according to an eight-site exchange model, composed of the two- and four-site exchange models as shown in Figures 5 and 12, respectively. From the best-fit simulations, shown in Figure 14, the distribution of flip angles and the fluctuating angles, (σ, ζ), are determined to be (25°, 10°) and (35°, 12°) at 27 and 90 °C, respectively.

Simulations by Flip Angle Distribution and Fluctuation of Chain Axis. From the simulation of the C6 carbon, it is found that the chain axis fluctuates. The simulations of the C4 CSA spectra are again carried out by considering the fluctuational motion. Figure 15 shows the best-fit simulations under the combined motions of phenylene ring flip and main-chain fluctuation. The parameter set of (σ, ζ) determined by these simulations are (25°, 15°) and (30°, 20°) at 27 and 90

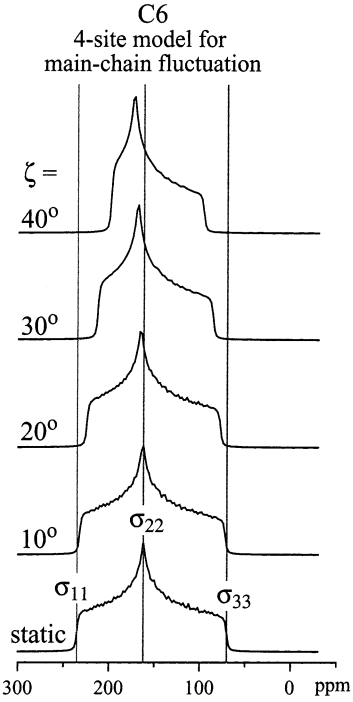

Figure 13. Simulated ^{13}C CSA spectra of C6 carbons under the fluctuational motion of phenylene ring axes in the fast limit. The cone angles of the motion, ζ (see Figure 12), are indicated in the figure. The simulated static CSA spectrum is also shown for reference.

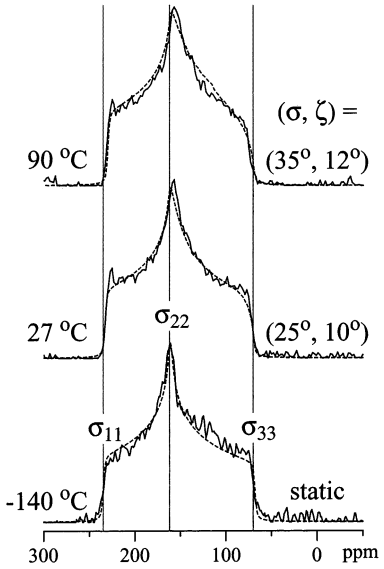

Figure 14. Experimental and simulated ^{13}C CSA spectra of C6 carbons at different temperatures. The simulations are carried out based on the eight-site exchange model. The parameter sets of (σ, ζ) = (25°, 10°) and (35°, 12°) are obtained from the best-fit simulations for 27 and 90 °C, respectively.

°C, respectively. These values are in good accord with those obtained from the C6 carbon.

Although the simulated spectra in Figure 15 are better than those in Figure 8, the main-chain fluctuation cannot be determined uniquely from the temperature dependence of CSA line shapes of the phenylene ring C−H carbons. The CSA spectra of the phenylene ring quaternary C3 and C6 carbons thus provide quantitative information on the main-chain fluctuation. This is crucial in the present experiments, as shown in the Discussion Section. The dynamics of quaternary carbons

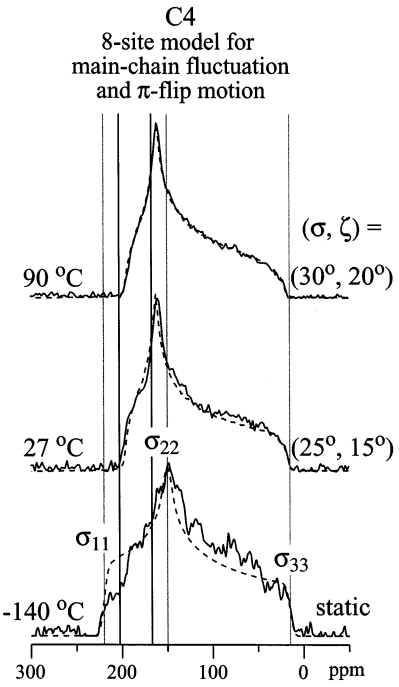

Figure 15. Experimental and simulated ^{13}C CSA spectra of C4 carbons at different temperatures. The simulations are carried out based on the eight-site exchange model. The parameter sets of (σ, ζ) = (25°, 15°) and (30°, 20°) give the best-fit simulations for 27 and 90 °C, respectively.

cannot be revealed directly by ^2H and C−H dipolar experiments. The small-angle main-chain fluctuation would be hard to detect by other CSA separation techniques[4,5,7−14] because all of them scale CSA spectra.

Note that the distribution of flip angles, σ, is consistent in Figures 8 and 15. This indicates that the flip angle of π-flip motion can be uniquely determined without considering the effect of main-chain fluctuational motion.

Analyses of CSA Line Shapes of the Other Carbons. Up to now, the temperature dependences of CSA patterns have been analyzed for phenylene ring carbons. For the other carbons species (C1, C2, C7/8), the CSA patterns are narrow, and quantitative analyses were difficult as found from Figures 3 and 4. Here, only the qualitative estimations were carried out for C2 and C7/8 carbons. For the C1 carbon, a satisfactory CSA line shape cannot be obtained at −140 °C because the intensity is quite small as shown in Figure 1a and the ω_1-projection in Figure 4b. The decrease in the methyl signal intensity at low temperature is also observed for BPA-PC, probably due to the decrease in CP or ^1H dipolar decoupling efficiencies.[33,34] The wiggles of a large and sharp C2 resonance line in the ω_1 dimension will also smear out the C1 CSA line shape. Figure 16 shows the temperature dependences of CSA line shapes for C2 and C7/8 carbons. For the C2 carbon, the CSAs at 27 and 90 °C are slightly narrower than that at −140 °C. This is consistent with the results of fluctuation of the main chain as described above. Although the resonance lines are overlapped for the C7 and C8 carbons, the narrowing of the CSA line shapes is observed with increasing temperature. From the detailed analysis by ^2H NMR,[24] a dynamics different from that of the bisphenol A residues was found to occur for these CH and CH_2 carbons.

Dynamics above the Glass Transition Temperature. The 2D MAT experiments between 90 and 150

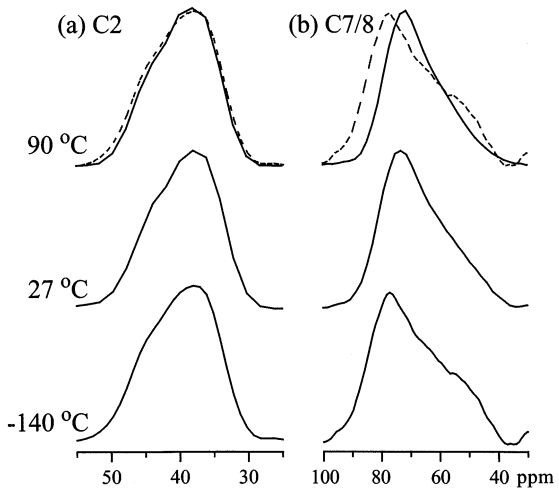

Figure 16. Experimental ^{13}C CSA spectra of C2 and C7/8 carbons at different temperatures. For clear comparison, the spectra at −140 °C overlapping to those at 90 °C are shown as broken lines.

°C are of interest for the characterization of main-chain motion. In the temperature range between 100 and 140 °C, however, analyzable 2D MAT spectra were not obtained due to the motional broadenings and the bad signal-noise ratio (see Figures 1 and 2 and ref 1). A much more serious problem is that the main-chain motion during the 1/3-rotation in the MAT experiments disturbs the averaging of chemical shift anisotropy in the MAT techniques. Therefore, we know from Figure 2 only that all the carbons locally undergo almost isotropic random orientational motion above 150 °C and exhibit some motional anisotropy at 130 °C with a rate above 10^5 Hz.

Discussion

Consistency with Previous Data. From the analyses of the ^{13}C CSA of PHR, the values of (σ, ζ) are determined to be (25°, 10−15°) and (30−35°, 12−20°) at 27 and 90 °C, respectively. Shi et al.[24] assumed the angular distribution of π-flip motion to be constant, σ = 25°, in the analyses of ^2H NMR spectra between −20 and 70 °C. Our results, σ = 25−35° at 27−90 °C, confirm that their assumption is reasonable, although a temperature dependence seems to exist. Poliks et al.[35] estimated the amplitude of main-chain motion in PHR from the dipolar spinning sideband pattern of the CH_3 carbons. From a comparison with crystalline bisphenol A as a model sample in the rigid state, the small-angle main-chain motion at room temperature is determined to be ζ = 10° from the CH_3 carbons. This is also consistent with our data of ζ = 10−15° at 27 °C.

Comparison with BPA-PC. Because of the excellent mechanical properties of BPA-PC, many research studies have been carried out to reveal the origin of the properties and γ-relaxation. Here, we compare the results for PHR obtained in this paper with those for BPA-PC. In the earlier work on BPA-PC, the distribution of the flip angle in the π-flip motion was not considered in the analyses of the C−H dipolar, ^{13}C CSA, and ^2H NMR experiments.[36−39] Only the ideal π-flips were considered. However, the flip angle was directly measured by 2D ^2H exchange NMR at −40 °C,[32] and the existence of flip angle distribution was proven to be correct. The Gaussian width of 50°[32] is translated into σ = 25° in our definition, which agrees with our results.

Because the CP/MAS resonance lines of carbonyl carbons and two kinds of quaternary carbons in the phenylene rings are overlapped in BPA-PC, the small-angle fluctuation of the main chain is hard to detect. However, it can be monitored through the CH_3 groups because this motion is considered to reflect the main-chain motion. The main-chain fluctuation was not observed by ^2H NMR spectra of CH_3-deuterated BPA-PC as clearly described in ref 39. In contrast, analyses of the C−H dipolar sideband spectra of the CH_3 groups show the 9−15° main-chain motion.[36] From the temperature dependence of the CSA line shapes of quaternary carbons in the phenylene rings of ^{13}C-labeled BPA-PC, the slopes of σ_{11} show an upfield shift with increasing temperature.[40] The slopes of σ_{11} at the 27 °C shift upfield by about 3 ppm compared to those at −138 °C, which is consistent with our results shown in Figure 11. The purpose of the study in ref 40 is not the dynamics of BPA-PC, but this also confirms the existence of the main-chain fluctuation. From these results, the phenylene ring and main-chain motions of bisphenol A residues in PHR and BPA-PC are found to be quite similar below the T_g of PHR.

Intermolecular Cooperative Motion: Open Gate Model. Here, we describe a model for intermolecular cooperative motion in PHR and BPA-PC based on their main-chain fluctuations. The apparent activation energies for the γ-relaxation were determined to be 54−56 kJ mol^{-1} by the mechanical relaxation analysis of BPA-PC.[41,42] These values are consistent with those for the π-flip motion of phenylene groups: 48 kJ mol^{-1} by the ^2H NMR experiments of PHR,[24] 51 kJ mol^{-1} by 1D and 2D CP/MAS experiments of PHR,[1] and 50 kJ mol^{-1} by the ^{13}C chemical shift anisotropy (CSA) experiments of BPA-PC.[37] Our model proposed here accounts for the simultaneous occurrence of phenylene ring and similar activation energies of phenylene ring π-flip motion and γ-relaxation.[1,24,41,43]

In solution, the phenylene rings undergo free rotations.[44] The conformational calculation of a single BPA-PC chain[45] also shows that the phenylene rings of isolated single BPA-PC chains nearly freely rotate around the phenylene ring axis at room temperature. In contrast, in the glassy state, the phenylene rings undergo distributed π-flip motion as described above. This is obviously due to the effect of intermolecular packing. Astonishingly, the local packing of BPA-PC is denser than that of the model crystalline compounds, which is confirmed by several solid-state NMR results by Schaefer et al.[46−50] To undergo π-flip motion in such a well-packed matrix, the adjacent polymer chains should move to lengthen the interchain distances and to create space for the flips. In other words, π-flip motion can occur only when the "gate" opens.

In the static case, the "gate" closes. The phenylene rings undergo a small-angle oscillational motion around the energy minimum. The amplitude of phenylene ring oscillational motion sometimes becomes large. The rings then thrust off the neighboring chains, and by this force, they move so as to open the "gate". During opening of the "gate", the phenylene rings can flip. After a π-flip motion, the "gate" closes and the phenylene rings are again in the energetically stable state. Because the "gate" will open only for the phenylene rings to flip, the

displacements of the neighboring chains would be small as has been experimentally determined ($\zeta = 10-12°$).

According to this model, phenylene ring motion activates the main-chain motion, and the main-chain motion in turn makes the ring flip. This would be the reason why the phenylene ring π-flip motion appears at the temperature of γ-relaxation and has almost the same activation energy as that of γ-relaxation, although the phenylene ring π-flip motion itself is not mechanically active. The strain under deformation could be relaxed though the cooperative interchain motion, which would induce the γ-relaxation.

In this model, the frequencies of main-chain fluctuational motion and phenylene ring motion should coincide. Because the amplitude of the main-chain fluctuational motion is small, the frequency is difficult to determine quantitatively. However, the following experimental and computer-simulated data support our model.

Schaefer et al. observed the decrease in ^{1}H T_2 values of BPA-PC and PHR by applying hydrostatic pressure.[51] The results suggest that the tighter interchain packing resulting from hydrostatic pressure suppresses molecular motion in BPA-PC and PHR, which is also compatible with our "open-gate" model. The magnitude of the pressure dependence in the NMR experiments was found to be comparable to the pressure variation in the γ-mechanical relaxation loss peak in BPA-PC.

This "open-gate" model is further consistent with generalized Langevin and Brownian dynamics simulations by Yaris et al.[52,53] Their simulation results clearly show that phenylene ring π-flips occur only when the distance between the phenylene ring and its nearest-neighbor chains increases by ~0.5 Å. In the case of a rigid lattice, the rings demonstrate little π-flips. Note that in their simulations the parallel interchain packing of phenylene rings is assumed on the basis of a bundle model. This bundle model was proposed by Schaefer et al.[46,47,49,50] on the basis of several interchain distance measurements by solid-state NMR. In the bundle, the polymer chains are aligned parallel, and no interchain displacements are found along the chain axis. Therefore, the intermolecular cooperative motion, proposed by Schaefer et al.[46,47,49,50] and Yaris et al.,[52,53] is the cooperative phenylene ring motion among the neighboring rings. In contrast, Jho and Yee[42] pointed out the problems in the bundle model, and according to Mitchell,[54] the parallel packing of the chains is considered to be less probable on the basis of his X-ray results. More random interchain orientations have been experimentally observed by 2D solid-state spin-diffusion NMR spectroscopy by Robyr et al.[55] The inconsistency of the results of Schaefer et al. and Robyr et al. would originate from the fact that Schaefer et al. measured the intermolecular distances. They only assumed the orientational correlation from these distances. In contrast, Robyr et al. measured the orientational correlation directly. Our "open-gate" model does not assume the existence of bundles. We consider only the experimentally confirmed results, the main-chain fluctuational motion, and the short interchain distances. Therefore, our model does not matter the interchain orientation and translational displacement. The point of the cooperative motion in our model is the fluctuation of neighboring chains due to the flip motion of the phenylene ring rather than the cooperative ring motion. The main-chain flexibility and close interchain packing are considered to be crucial factors for the γ-relaxation. Too rigid chains would suppress π-flips. Loose interchain packing would not activate the main-chain motion.

Effect of Intrachain Cooperativity. Yee et al.[42,56] investigated the intramolecular cooperative motion from the mechanical relaxations of copolymers and concluded that the intramolecular cooperativity is the origin of γ-relaxation. They considered that the linkage between intrachain neighboring bisphenol A segments plays an important role in motional cooperativity; a flexible linkage provides less cooperativity. From the dynamic mechanical analyses (DMA) of copolymers of BPA-PC and tetramethylbisphenol A PC (TMBPA-PC),[42] where the linkage is $-O-C(=O)-O-$, they concluded that the γ-relaxation of BPA-PC originates from the intrachain cooperative motion of several repeating units. In contrast, the γ-relaxation of copolyformals of BPA (BPA-PF) and TMBPA (TMBPA-PF), where the linkage is $-O-CH_2-O-$, is not dependent on the block length of the BPA segments. This indicates that no intrachain cooperative motion exists in BPA-PF,[56] and they concluded that the γ-relaxation of BPA-PF does not require long-range in-chain cooperativity. If in-chain cooperative motion is the origin of the γ-relaxation, the relaxation should not be observed for BPA-PF because individual motions of the constituent groups are unable to induce the mechanical relaxation. However, the tan δ value in BPA-PF is comparable to that in BPA-PC in their own work.[41,56] Therefore, the γ-relaxation behavior cannot be explained only by the intramolecular cooperative motion. In the present case also, the linkage of PHR ($-O-CH_2-CH(-OH)-CH_2-O-$) is more flexible than those of BPA-PC and BPA-PF. However, the tan δ peak of PHR is quite similar to those for BPA-PC and BPA-PF.[3,41,56] The results of similar tan δ values in these polymers are more consistent with the results in which the amplitudes of main-chain motions are independent of the linkages. Therefore, we think that the intermolecular cooperative motion described by the "open-gate" model is crucial for the subrelaxation in PHR and BPA-PC.

Conclusions

The dynamics of amorphous poly(2-hydroxypropyl ether of bisphenol A) (PHR), quenched from the melt, has been investigated by two-dimensional solid-state ^{13}C magic angle turning (MAT) NMR spectroscopy. The chemical shift anisotropy (CSA) powder patterns of the respective ^{13}C species are separately obtained by the experiments from −140 to 90 °C. On the basis of the temperature dependence of the CSA line shapes of phenylene ring quaternary carbons, the main-chain of PHR is found to fluctuate, which cannot be measured by ^{2}H NMR measurements. The CSA line shapes of phenylene ring C−H carbons show that the rings undergo a flip motion simultaneously with the main-chain fluctuation. The quantitative analyses of these CSA line shapes reveal that (1) the phenylene rings undergo a π-flip motion with standard deviations, σ, of 25 and 30−35° and (2) the cone angle of the main-chain fluctuation is 10−15 and 12−20° at 27 and 90 °C, respectively.

On the basis of the main-chain motion, we propose a model to account for the coincidence of the frequencies and the activation energies of phenylene ring π-flip motion and γ-relaxation. In this model, the phenylene rings in the process of π-flip motion make a thrust at

the neighboring chains, which activates the main-chain fluctuational motion. The similar time scales and the activation energies of phenylene ring motion and mechanical relaxation are not considered to be accidental. These two processes will be related by such an interchain cooperative process.

The mechanical γ-relaxations in PHR and bisphenol A polycarbonate (BPA-PC) are similar. The present NMR experiments also show similar low-temperature dynamics in PHR and BPA-PC. These results indicate that the low-temperature dynamics in these polymers does not depend on the linkage group between neighboring bisphenol A residues, $-O-CH_2-CH(-OH)-CH_2-O-$ and $-O-C(=O)-O-$. Therefore, the mechanical γ-relaxation is not considered to originate from the intrachain cooperative motion. Otherwise, a more flexible linkage group in PHR has less intrachain motional cooperativity, which results in lower γ-relaxation.

From the 1D CSA measurements, the main-chain motion is still found to be anisotropic at 130 °C. At 150 °C, the main chains locally undergo almost isotropic random orientational motion with a rate above 10^5 s^{-1}.

Acknowledgment. The authors thank Mr. Ninomiya of UBE Science Co., Ltd., for providing the phenoxy resin pellets.

References and Notes

(1) Kaji, H.; Tai, T.; Horii, F. *Macromolecules* **2001**, *34*, 6318.
(2) Takahama, T.; Geil, P. H. *J. Polym. Sci., Polym. Phys. Ed.* **1982**, *20*, 1979.
(3) Erro, R.; Gaztelumendi, M.; Nazabal, J. *J. Polym. Sci., Part B: Polym. Phys. Ed.* **1996**, *34*, 1055.
(4) Zeigler, R. C.; Wind, R. A.; Maciel, G. E. *J. Magn. Reson.* **1988**, *79*, 299.
(5) Bax, A.; Szeverenyi, N. M.; Maciel, G. E. *J. Magn. Reson.* **1983**, *52*, 147.
(6) Gan, Z. *J. Am. Chem. Soc.* **1992**, *114*, 8307.
(7) Terao, T.; Fujii, T.; Onodera, T.; Saika, A. *Chem. Phys. Lett.* **1984**, *107*, 145.
(8) Bax, A.; Szeverenyi, N. M.; Maciel, G. E. *J. Magn. Reson.* **1983**, *55*, 494.
(9) Iwamiya, J. H.; Davis, M. F.; Maciel, G. E. *J. Magn. Reson.* **1990**, *88*, 199.
(10) Horii, F.; Beppu, T.; Takaesu, N.; Ishida, M. *Magn. Reson. Chem.* **1994**, *32*, S30.
(11) Horii, F.; Uyeda, T.; Beppu, T.; Murata, T.; Odani, H. *Bull. Inst. Chem. Res., Kyoto Univ.* **1992**, *70*, 198.
(12) Frydman, L.; Chingas, G. C.; Lee, Y. K.; Grandinetti, P. J.; Eastman, M. A.; Barrall, G. A.; Pines, A. *J. Chem. Phys.* **1992**, *97*, 4800.
(13) Tycko, R.; Dabbagh, G.; Mirau, P. A. *J. Magn. Reson.* **1989**, *85*, 265.
(14) Liu, S. F.; Mao, J. D.; Schmidt-Rohr, K. *J. Magn. Reson.* **2002**, *155*, 15.
(15) Hu, J. Z.; Orendt, A. M.; Alderman, D. W.; Pugmire, R. J.; Ye, C. H.; Grant, D. M. *Solid State Nucl. Magn. Reson.* **1994**, *3*, 181.
(16) Hu, J. Z.; Wang, W.; Liu, F.; Solum, M. S.; Alderman, D. W.; Pugmire, R. J.; Grant, D. M. *J. Magn. Reson. A* **1995**, *113*, 210.
(17) Hu, J. Z.; Wang, W.; Bai, S.; Pugmire, R. J.; Taylor, C. M. V.; Grant, D. M. *Macromolecules* **2000**, *33*, 3359.
(18) Hu, J. Z.; Taylor, C. M. V.; Pugmire, R. J.; Grant, D. M. *J. Magn. Reson.* **2001**, *152*, 7.
(19) Kaji, H.; Horii, F. *J. Chem. Phys.* **1998**, *109*, 4651.
(20) Kaplan, M. L.; Bovey, F. A.; Chang, H. V. *Anal. Chem.* **1975**, *47*, 1703.
(21) Tsuji, H.; Horii, F.; Nakagawa, M.; Ikada, Y.; Odani, H.; Kitamaru, R. *Macromolecules* **1992**, *25*, 4114.
(22) Bielecki, A.; Burum, D. P. *J. Magn. Reson. A* **1995**, *116*, 215.
(23) Takahashi, T.; Kawashima, H.; Sugisawa, H.; Baba, T. *Solid State Nucl. Magn. Reson.* **1999**, *15*, 119.
(24) Shi, J.-F.; Inglefield, P. T.; Jones, A. A.; Meadows, M. D. *Macromolecues* **1996**, *29*, 605.
(25) Cohen Addad, J. P.; Guillermo, A. *J. Chem. Phys.* **1999**, *111*, 7131.
(26) Cohen Addad, J. P.; Guillermo, A. *Phys. Rev. Lett.* **2000**, *85*, 3432.
(27) Guillermo, A.; Cohen Addad, J. P.; Bytchenkoff, D. *J. Chem. Phys.* **2000**, *113*, 5098.
(28) Guillermo, A.; Cohen Addad, J. P. *J. Chem. Phys.* **2002**, *116*, 3141.
(29) Cohen Addad, J. P.; Guillermo, A. *Macromolecules* **2003**, *36*, 1609.
(30) Ernst, R. R.; Bodenhausen, G.; Wokaun, A. *Principles of Nuclear Magnetic Resonance in One and Two Dimensions*; Clarendon Press: Oxford, 1987.
(31) Schmidt-Rohr, K.; Spiess, H. W. *Multidimensional Solid-State NMR and Polymers*; Academic Press: London, 1994.
(32) Hansen, M. T.; Blumich, B.; Boeffel, C.; Spiess, H. W.; Morbitzer, L.; Zembrod, A. *Macromolecules* **1992**, *25*, 5542.
(33) Henrichs, P. M.; Linder, M.; Hewitt, J. M.; Massa, D.; Isaacson, H. V. *Macromolecules* **1984**, *17*, 2412.
(34) Garroway, A. N.; VanderHart, D. L.; Earl, W. L. *Philos. Trans. R. Soc. London, Ser. A* **1981**, *299*, 609.
(35) Poliks, M. D.; Gullion, T.; Schaefer, J. *Macromolecules* **1990**, *23*, 2678.
(36) Schaefer, J.; Stejskal, E. O.; McMay, R. A.; Dixson, W. T. *Macromolecules* **1984**, *17*, 1479.
(37) Roy, A. K.; Jones, A. A.; Inglefield, P. T. *Macromolecules* **1986**, *19*, 1356.
(38) Wehrle, M.; Hellmann, G. P.; Spiess, H. W. *Colloid Polym. Sci.* **1987**, *265*, 815.
(39) Spiess, H. W. *Colloid Polym. Sci.* **1983**, *261*, 193.
(40) Tomaselli, M.; Robyr, P.; Meier, B. H.; Grob-Pisano, C.; Ernst, R. R.; Suter, U. W. *Mol. Phys.* **1996**, *89*, 1663.
(41) Yee, A. F.; Smith, S. A. *Macromolecues* **1981**, *14*, 54.
(42) Jho, J. Y.; Yee, A. F. *Macromolecules* **1991**, *24*, 1905.
(43) The γ-relaxation for PHR was observed in a temperature region centered at −70 °C,[2,3,24] which was slightly higher than the temperature range of the π-flip motion in PHR. This is due to the overlap of trans−gauche isomerization of hydroxy ether groups in PHR.[24]
(44) Schaefer, J.; Stejskal, E. O.; Buchdahl, R. *Macromolecules* **1977**, *10*, 384.
(45) Schaefer, J.; Stejskal, E. O.; Perchak, D.; Skolnick, J.; Yaris, R. *Macromolecules* **1985**, *18*, 368.
(46) Schmidt, A.; Kowalewski, T.; Schaefer, J. *Macromolecules* **1993**, *26*, 1729.
(47) Lee, P. L.; Schaefer, J. *Macromolecules* **1995**, *28*, 1921.
(48) Lee, P. L.; Kowalewski, T.; Poliks, M. D.; Schaefer, J. *Macromolecules* **1995**, *28*, 2476.
(49) Klug, C. A.; Zhu, W.; Tasaki, K.; Schaefer, J. *Macromolecules* **1997**, *30*, 1734.
(50) Lee, P. L.; Schaefer, J. *Macromolecules* **1992**, *25*, 5559.
(51) Walton, J. H.; Lizak, M. J.; Conradi, M. S.; Gullion, T.; Schaefer, J. *Macromolecules* **1990**, *23*, 416.
(52) Whitney, D. R.; Yaris, R. *Macromolecules* **1997**, *30*, 1741.
(53) Perchak, D.; Skolnick, J.; Yaris, R. *Macromolecules* **1987**, *20*, 121.
(54) Mitchell, G. R. In *Order in the Amorphous State of Polymers*; Keinath, S. E., Miller, R. C., Rieke, J. K., Eds.; Plenum: New York, 1987; pp 1−31.
(55) Robyr, P.; Gan, Z.; Suter, U. W. *Macromolecules* **1998**, *31*, 6199.
(56) Li, L.; Yee, A. F. *Macromolecules* **2002**, *35*, 425.

MA0300342